Ultrahigh-energy neutrino fluxes and their constraints

Oleg E. Kalashev,[1] Vadim A. Kuzmin,[1] Dmitry V. Semikoz,[1,2] and Günter Sigl[3]
[1]*Institute for Nuclear Research of the Academy of Sciences of Russia, Moscow 117312, Russia*
[2]*Max-Planck-Institut für Physik (Werner-Heisenberg-Institut), Föhringer Ring 6, 80805 München, Germany*
[3]*GReCO, Institut d'Astrophysique de Paris, C.N.R.S., 98 bis boulevard Arago, F-75014 Paris, France*
(Received 12 May 2002; published 12 September 2002)

Applying our recently developed propagation code we review extragalactic neutrino fluxes above 10^{14} eV in various scenarios and how they are constrained by current data. We specifically identify scenarios in which the cosmogenic neutrino flux above $\simeq 10^{18}$ eV, produced by pion production of ultrahigh energy cosmic rays outside their sources, is considerably higher than the ''Waxman-Bahcall bound.'' This is easy to achieve for sources with hard injection spectra and luminosities that were higher in the past. Such fluxes would significantly increase the chances to detect ultrahigh energy neutrinos with experiments currently under construction or in the proposal stage.

DOI: 10.1103/PhysRevD.66.063004 PACS number(s): 98.70.Sa, 95.85.Ry, 98.70.Vc, 98.80.−k

I. INTRODUCTION

The farthest source observed so far in neutrinos was supernova SN 1987A from which about 20 neutrinos in the 10–40 MeV range were detected [1]. Extraterrestrial neutrinos of much higher energy are usually expected to be produced as secondaries of cosmic rays interacting with ambient matter and photon fields and should thus be associated with cosmic ray sources ranging from our Galaxy to powerful active galactic nuclei (AGN) [2]. Traditional neutrino telescopes now under construction aim to detect such neutrinos up to $\sim 10^{16}$ eV by looking for showers and/or tracks from charged leptons produced by charged current reactions of neutrinos in ice, in the case of the Antarctic Moon and Neutrino Detector Array (AMANDA) [3,4] and its next generation version ICECUBE [5], in water, in the case of BAIKAL [6,7], ANTARES [9], and NESTOR [10], or underground, in the case of MACRO [11] (for recent reviews of neutrino telescopes see Ref. [12]).

On the other hand, the problem of the origin of the cosmic rays themselves is still unsolved, especially at ultrahigh energies (UHE) above $\simeq 4\times 10^{19}$ eV, where they lose energy rapidly by pion production and pair production (protons only) on the cosmic microwave background (CMB) [13,14]. For sources farther away than a few dozen Mpc this would predict a break in the cosmic ray flux known as Greisen-Zatsepin-Kuzmin (GZK) cutoff [15], around 50 EeV. This break has not been observed by experiments such as Fly's Eye [16], Haverah Park [17], Yakutsk [18] and the Akenco Grant Air Showers Array (AGASA) [19], which instead show an extension beyond the expected GZK cutoff and events above 100 EeV (however, the new experiment HiRes [20] currently seems to see a cutoff in the monocular data [21]). This has led to the current construction of the southern site of the Pierre Auger Observatory [22], a combination of an array of charged particle detectors with fluorescence telescopes for air showers produced by cosmic rays above $\sim 10^{19}$ eV which will lead to about a hundred-fold increase of data. The telescope array, another planned project based on the fluorescence technique, may serve as the optical component of the northern Pierre Auger site planned for the future [23]. There are also plans for space based observatories such as EUSO [24] and OWL [27] of even bigger acceptance. These instruments will also have considerable sensitivity to neutrinos above $\sim 10^{19}$ eV, typically from the near-horizontal air-showers that are produced by them [28]. Furthermore, the old Fly's Eye experiment [29] and the AGASA experiment [30] have established upper limits on neutrino fluxes based on the nonobservation of horizontal air showers.

In addition, there are plans to construct telescopes to detect fluorescence and Čerenkov light from near-horizontal showers produced in mountain targets by neutrinos in the intermediate window of energies between $\sim 10^{15}$ eV and $\sim 10^{19}$ eV [31,32]. The alternative of detecting neutrinos by triggering onto the radio pulses from neutrino-induced air showers is also investigated currently [33]. Two implementations of this technique, RICE, a small array of radio antennas in the South pole ice [34], and the Goldstone Lunar Ultrahigh energy neutrino Experiment (GLUE), based on monitoring of the moons rim with the NASA Goldstone radio telescope for radio pulses from neutrino-induced showers [35], have so far produced neutrino flux upper limits. Acoustic detection of neutrino induced interactions is also being considered [36].

The neutrino detection rates for all future instruments will crucially depend on the fluxes expected in various scenarios. The flux of ''cosmogenic'' neutrinos created by primary protons above the GZK cutoff in interactions with CMB photons depends both on the primary proton spectrum and on the location of the sources. The cosmogenic neutrino flux is the only one that is guaranteed to exist just by the observations of ultrahigh energy cosmic rays (UHECRs) and was studied soon after the discovery of the CMB [37]. Note, however, that there is no firm lower bound on the cosmogenic neutrino flux if the UHECR sources are much closer than the GZK distance.

If sources are located beyond the GZK distance and the proton flux extends beyond the GZK cutoff, the neutrino fluxes can be significant. This possibility is favored by the lack of nearby sources and by the hardening of the cosmic ray spectrum above the ''ankle'' at $\simeq 5\times 10^{18}$ eV. It is also

suggested by possible correlations of UHECR arrival directions with compact radio quasars [38] and more significant correlations with BL Lacertae objects [39], some of which are possibly also luminous in GeV γ rays [40] and at distances too large to be consistent with the absence of the GZK cutoff.

Whereas roughly homogeneously distributed proton sources can naturally explain the UHECR flux below the GZK cutoff (see, e.g., Refs. [41] and [42]), the highest energy events may represent a new component. They may be new messenger particles, which propagate through the Universe without interacting with the CMB [43], or may have originated as extremely high energy ($E \gtrsim 10^{23}$ eV) photons, which can propagate several hundred Mpc (constantly losing energy) and can create secondary photons inside the GZK volume [42]. Decaying super-heavy relics from the early Universe (see Refs. [14,44] for reviews) can also explain UHECRs and predict UHE neutrino fluxes detectable by future experiments.

Another speculative possibility is to explain UHECRs beyond the GZK cutoff by the UHE protons and photons from decaying *Z*-bosons produced by UHE neutrinos interacting with the relic neutrino background [45]. The big drawback of this scenario is the need for enormous primary neutrino fluxes that cannot be produced by known astrophysical acceleration sources without overproducing the GeV photon background [46], and thus it most likely requires a more exotic top-down type source such as X particles exclusively decaying into neutrinos [47]. As will be shown in Sec. VI, even this possibility is also significantly constrained by existing measurements.

Active galactic nuclei (AGN) can be sources of neutrinos if protons are accelerated in them [2]. In the present paper we consider only the two representative limits of low and high optical depth for pion (and neutrino) production in the source. In the first case the protons accelerated in the AGN freely escape and neutrinos are produced only in interactions with the CMB (cosmogenic neutrinos). For the second case we discuss an example of possible high neutrino fluxes from a non-shock acceleration AGN model [49], in which primary protons lose all their energy and produce neutrinos directly in the AGN core.

Motivated by the increased experimental prospects for ultrahigh energy neutrino detection, in the present paper we reconsider flux predictions in the above scenarios with our recently combined propagation codes [42,46,50,51]. Our main emphasise is thereby on model independent flux ranges consistent with all present data on cosmic and γ rays. For any scenario involving pion production the fluences of the latter are comparable to the neutrino fluences. However, electromagnetic (EM) energy injected above $\sim 10^{15}$ eV cascades down to below the pair production threshold for photons on the CMB, and EM energy above 100 GeV also cascades down due to the pair production on the infrared/optical background. The resulting intensity and spectrum of γ rays below 100 GeV are rather insensitive to these backgrounds [14,52]. The cascade thus gives rise to a diffuse photon flux in the GeV range which is constrained by the flux observed by the EGRET instrument on board the Compton γ-ray observatory [53]. For all neutrino flux scenarios the related γ-ray and cosmic ray fluxes have to be consistent with the EGRET and cosmic ray data, respectively.

Section II summarizes the numerical technique used in this paper. In Sec. III we discuss the cosmogenic neutrino flux and its dependence on various source characteristics. We specifically find an upper limit considerably higher than typical fluxes in the literature and remark why it is higher than the Waxman-Bahcall (WB) [54] and even the Mannheim-Protheroe-Rachen (MPR) [55] bounds for sources transparent to cosmic and γ rays. In Sec. IV we review neutrino flux predictions in top down scenarios where UHECRs are produced in decays of super-massive particles continuously released from topological defect relics from the early Universe. Section V discusses neutrino fluxes in scenarios where the cosmic rays observed at the highest energies are produced as secondaries of these neutrinos from interactions with the relic cosmological neutrino background, often called *Z*-burst scenario. In Sec. VI we focus on a combination of top-down and *Z*-burst scenarios considered by Gelmini and Kusenko [47], namely super-heavy particles mono-energetically decaying exclusively into neutrinos (see, however, [48]). In Sec. VII we discuss possible high neutrino fluxes from a non-shock acceleration AGN model [49]. Finally, in Sec. VIII we conclude.

II. NUMERICAL TECHNIQUE

Our simulations are based on two independent codes that have extensively been compared down to the level of individual interactions. Both of them are implicit transport codes that evolve the spectra of nucleons, γ rays, electrons, electron-, muon-, and tau-neutrinos, and their antiparticles along straight lines. Arbitrary injection spectra and redshift distributions can be specified for the sources and all relevant strong, electromagnetic, and weak interactions have been implemented. For details see Refs. [46,50,51].

Relevant neutrino interactions for the *Z*-burst scenario are both the s-channel production of *Z* bosons and the t-channel production of *W* bosons. The decay products of the *Z* boson were taken from simulations with the [56] Monte Carlo event generator using the tuned parameter set of the OPAL Collaboration [57].

The main ambiguities in propagation of photons concern the unknown rms magnetic field strength *B* which can influence the predicted γ-ray spectra via synchrotron cooling of the electrons in the EM cascade, and the strength of the universal radio background (URB) which influences pair production by UHE γ rays [58]. Photon interactions in the GeV to TeV range are dominated by infrared and optical universal photon backgrounds (IR/O), for which we took the results of Ref. [59]. The resulting photon flux in the GeV range is not sensitive to details of the IR/O backgrounds.

Concerning the cosmology parameters we chose the Hubble parameter $H_0 = 70$ km s^{-1} Mpc^{-1} and a cosmological constant $\Omega_\Lambda = 0.7$, as favored today. These values will be used in all cases unless otherwise indicated.

For the neutrinos we assume for simplicity that all three flavors are completely mixed as suggested by experiments

[60] and thus have equal fluxes. For each flavor we sum fluxes of particles and antiparticles.

Predictions for all the fluxes in both codes agree within tens of percents. Only for the *Z*-burst scenarios do the photon fluxes agree only within a factor $\simeq 2$ between the two original codes due to the different implementation of *Z*-decay spectra and the ambiguities in photon propagation mentioned above. This difference has no influence on the conclusions of this paper.

In the present investigation we parametrize power law injection spectra of either protons (for UHECR sources) or neutrinos (for *Z*-burst models) per co-moving volume in the following way:

$$\phi(E,z) = f(1+z)^m E^{-\alpha} \Theta(E_{\max}-E) z_{\min} \leqslant z \leqslant z_{\max}, \quad (1)$$

where f is the normalization that has to be fitted to the data. The free parameters are the spectral index α, the maximal energy $E_{\max}$, the minimal and maximal redshifts $z_{\min}$, $z_{\max}$, and the redshift evolution index m. The resulting neutrino spectra depend insignificantly on $z_{\min}$ in the range $0 \leqslant z_{\min} \leqslant 0.1$ where local effects could play a role, and thus we will set $z_{\min}=0$ in the following.

To obtain the maximal neutrino fluxes for a given set of values for all these parameters, we determine the maximal normalization f in Eq. (1) by demanding that both the accompanying nucleon and γ-ray fluxes are below the observed cosmic ray spectrum and the diffuse γ-ray background observed by the Energetic Gamma Ray Experiment Telescope (EGRET), respectively.

III. THE COSMOGENIC NEUTRINO FLUX

A. Dependence on unknown parameters

In this section we discuss the case when primary UHECRs produce cosmogenic neutrinos as well as γ rays during propagation. For EM propagation we use $B=10^{-9}$ G and the intermediate URB strength estimate of Ref. [58]. These parameters only influence the γ-ray flux at UHEs, but not in the GeV range where the flux only depends on the total injected EM energy. Therefore, in this scenario the resulting neutrino fluxes are insensitive to the poorly known UHE γ-ray absorption because the ''visible'' UHE flux is always dominated by the primary cosmic rays and not by the secondary $\gamma-$ray flux, as can be seen in Figs. 9 and 10 below.

Figures 1, 2, 3, 4, and 5 show the dependences of the cosmogenic neutrino flux (average per flavor) for which associated cosmic and γ-ray fluxes are consistent with the data, on the maximal source redshift $z_{\max}$, maximal injection energy $E_{\max}$, redshift evolution index m, spectral power law index α, and cosmological parameters, respectively. In each figure the line for the highest neutrino flux corresponds to a significant contribution of the accompanying γ-ray flux to the observed flux at the EGRET region, whereas for the other lines the γ-ray flux gives negligible contributions to the EGRET flux.

Figure 2 shows that a change of the primary proton maximum energy changes the secondary neutrino flux only in the high energy region. The reason for this behavior is the shape

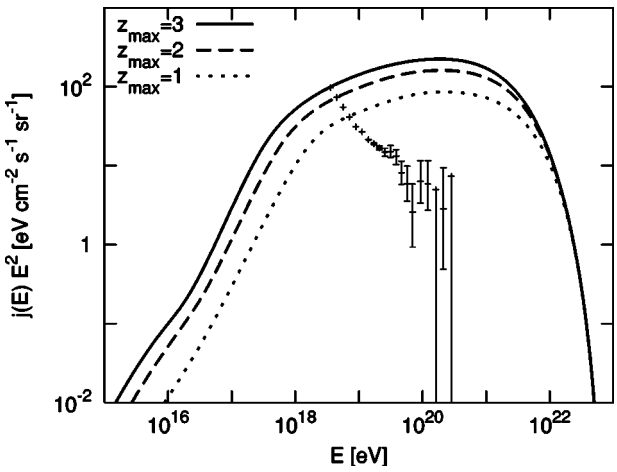

FIG. 1. Dependence of the average maximal cosmogenic neutrino flux per flavor consistent with all cosmic and γ-ray data on the maximal redshift $z_{\max}$, for the values indicated. Values assumed for the other parameters in Eq. (1) for proton primaries are $E_{\max}=10^{23}$ eV, $m=3$, $\alpha=1.5$. Also shown are the AGASA cosmic ray data above 3×10^{18} eV [19].

of the pion production cross section which at the lowest energies is dominated by the single pion Δ resonance. Figures 1 and 3 show that the cosmogenic neutrino flux at the lowest energies mostly depends on the maximum redshift $z_{\max}$ and the evolution index m. This is especially relevant for experiments with their main sensitivity below $\sim 10^{19}$ eV such as ICECUBE (see Fig. 10 below). Figure 4 shows that the maximal neutrino flux significantly increases with decreasing proton injection power law index. Figure 5 shows that the variation of the maximal neutrino flux with cosmology parameters Ω_Λ and H_0 is rather modest, about 50% for values discussed in recent years.

B. Active galactic nuclei as UHECR sources

Here we consider AGN sources for the primary UHECR flux, with the typical evolution parameters $m=3.4$ for z

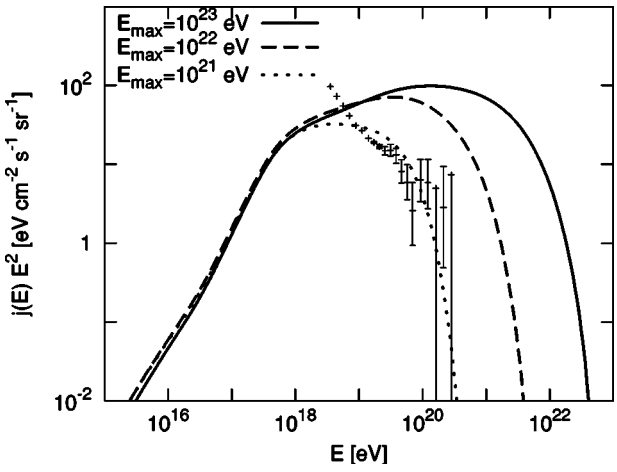

FIG. 2. Dependence of the average maximal cosmogenic neutrino flux per flavor consistent with all cosmic and γ-ray data on the maximal injection energy $E_{\max}$, for the values indicated. Values assumed for the other parameters are $z_{\max}=2$, $\alpha=1.5$, $m=3$. The cosmic ray data are as in Fig. 1.

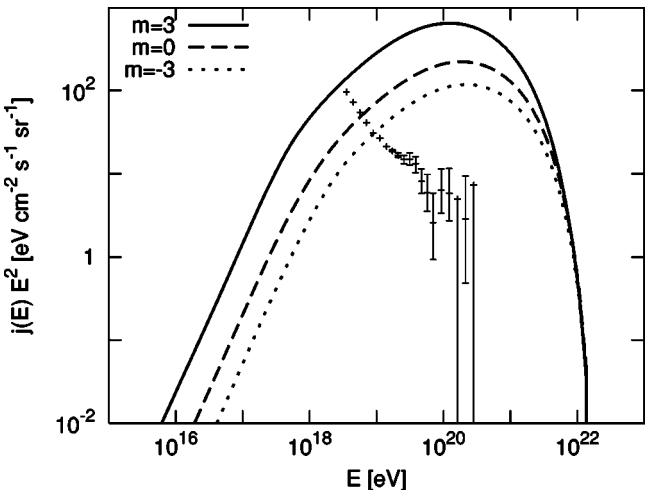

FIG. 3. Dependence of the average maximal cosmogenic neutrino flux per flavor consistent with all cosmic and γ-ray data on the source evolution index m, for the values indicated. Values assumed for the other parameters are $z_{\max}=2$, $E_{\max}=3\times10^{22}$ eV, $\alpha=1$. The cosmic ray data are as in Fig. 1.

<1.9 and $m=0$ for $1.9<z<2.9$ [61]. The only free remaining parameters are the power law index α and the maximum energy $E_{\max}$ for the proton injection spectrum, and the flux normalization f in Eq. (1). We first checked that for the case $\alpha=2$ we agree with the Waxman-Bahcall (WB) bound. Our cosmogenic neutrino fluxes agree reasonably well with the corresponding ones shown in Fig. 4 of Ref. [62] when taking into account maximal mixing assumed in the present paper.

Figure 6 shows the maximal cosmogenic neutrino flux for sources with hard spectra, $\alpha=1$, as a function of the maximal proton energy $E_{\max}$ and a mono-energetic injection spectrum at $E=3\times10^{21}$ eV. For the case $\alpha=1$, MPR [55] computed the sum of the cosmogenic neutrino flux and the neutrino flux directly emitted by the sources which are assumed to be transparent to neutrons. Our fluxes shown here

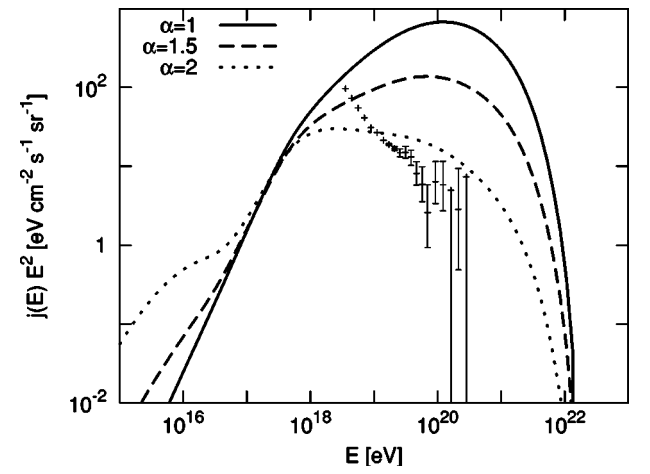

FIG. 4. Dependence of the average maximal cosmogenic neutrino flux per flavor consistent with all cosmic and γ-ray data on the injection spectrum power law index α, for the values indicated. Values assumed for the other parameters are $z_{\max}=2$, $E_{\max}=3\times10^{22}$ eV, $m=3$. The cosmic ray data are as in Fig. 1.

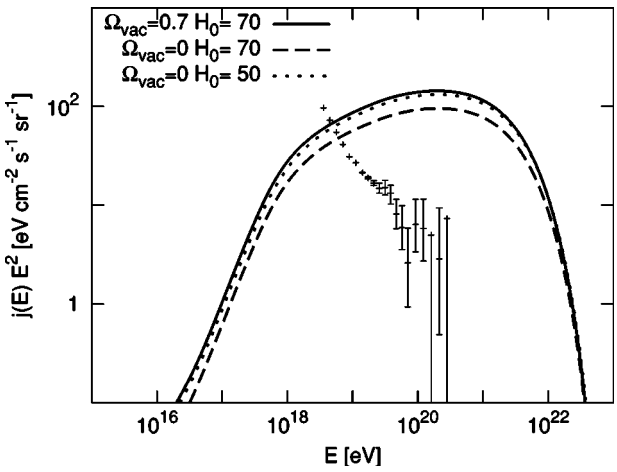

FIG. 5. Dependence of the average maximal cosmogenic neutrino flux per flavor consistent with all cosmic and γ-ray data on the cosmological vacuum energy density Ω_Λ and Hubble rate H_0, measured in $\mathrm{kms}^{-1}\mathrm{Mpc}^{-1}$, for the values indicated. Values assumed for the other parameters are $z_{\max}=2$, $E_{\max}=10^{23}$ eV, $\alpha=1.5$, $m=3$. The cosmic ray data are as in Fig. 1.

only include the cosmogenic flux. Nevertheless our fluxes overshoot the comparable MPR fluxes by up to a factor 5 at energies below the peak flux. This is most likely due to a combination of the different cosmology (see Fig. 5) and a different implementation of multi-pion production which influences interactions of nucleons at high energies, thus at high redshift and in turn the low energy tail of cosmogenic neutrinos.

Figure 6 and also Figs. 2–4 demonstrate in a general way that it is easy to exceed the WB bound and even the MPR bound for injection spectra harder than about E^{-2}. This is because Waxman-Bahcall restricted themselves to nucleon

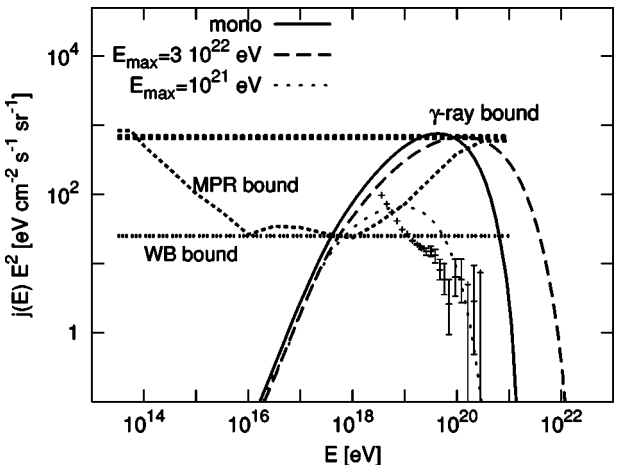

FIG. 6. Dependence of the average cosmogenic neutrino flux per flavor on maximum injection energy $E_{\max}$, for the values indicated, assuming $\alpha=1$ and the AGN evolution parameters discussed in the text. "mono" indicates mono-energetic proton injection at $E=3\times10^{21}$ eV. For comparison, the γ-ray bound derived from the EGRET GeV γ-ray flux [53], Eq. (2), the MPR limit for optically thin sources [55], and the WB limit for AGN-like redshift evolution [54] are also shown. The cosmic ray data are as in Fig. 1.

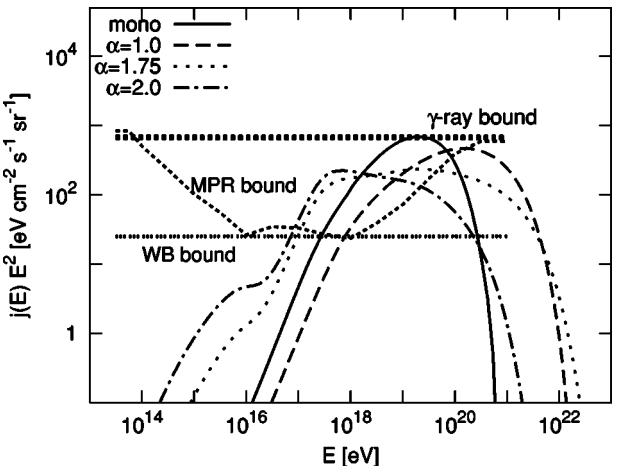

FIG. 7. Dependence of the average cosmogenic neutrino flux per flavor maximized over maximal injection energy $E_{\max}$, evolution index m, and normalization consistent with all cosmic and γ-ray data, on the injection spectrum power law index α. "mono" indicates mono-energetic proton injection at $E=10^{21}$ eV. The rest of the line key is as in Fig. 6.

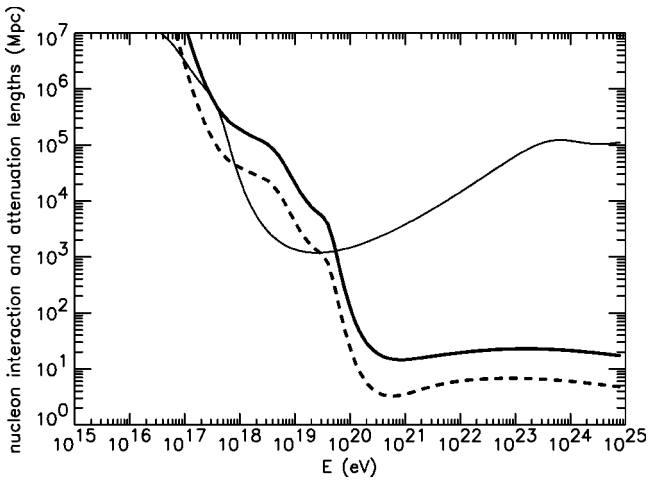

FIG. 8. The nucleon interaction length (dashed line) and energy attenuation length (solid line) for photo-pion production and the proton attenuation length for pair production (thin solid line) in the combined CMB and the estimated total extragalactic radio background intensity.

injection spectra softer than E^{-2} and sources smaller than nucleon interaction lengths [54]. Thus, their bound does not directly apply to the cosmogenic neutrino flux. In addition, in our opinion, their assumptions on the injection spectra are too narrow: Possible scenarios with hard injection spectra and the AGN redshift evolution assumed here (which is the same as the one used by Waxman-Bahcall) include cases where UHECRs are accelerated by the electromotive force produced by magnetic fields threading the horizons of spinning super-massive black holes in the centers of galaxies [63] or by reconnection events around forming galaxies [64].

In any scenario involving pion production for the creation of γ rays and neutrinos, the fluxes per flavor are approximately related by $F_\nu(E)\approx F_\gamma(E)/3$. Assuming smooth spectra and comparing with the EGRET γ-ray fluence, energy conservation implies

$$E^2F_\nu(E)\lesssim 6\times 10^2 \ \ \mathrm{eVcm^{-2}\,s^{-1}\,sr^{-1}}. \qquad (2)$$

This ultimate bound is also shown in Fig. 6 and Fig. 7 below. It corresponds to the MPR limit for optically thick sources. The maximal $E^2j(E)$ of the fluxes in Figs. 6 and 7 below indeed reach this γ-ray bound Eq. (2).

Note that the two theoretical bounds shown in Fig. 6 represent fluxes per neutrino flavor under the assumption of maximal neutrino mixing. They are thus about a factor 2 lower than in Refs. [54,55] which show muon neutrino fluxes in the absence of mixing where the tau-neutrinos fluxes are negligible and electron neutrino fluxes are about a factor 2 smaller. The WB and MPR bounds represent upper neutrino flux limits for compact sources such as AGN and γ-ray bursts in case of small optical depth for nucleons. We discuss a specific non-shock acceleration scenario in Sec. VII, for which both of the above bounds are not valid because the source optical depth for nucleons is large (for reviews on AGN neutrino fluxes see, e.g., Ref. [2]).

C. General case of arbitrary source evolution

In this section we consider more general UHECR sources and relax the restrictions on their redshift evolution. Figure 7 shows that cosmogenic neutrino fluxes higher than both the WB and MPR limits are possible even for relatively soft E^{-2} proton injection spectra, if the redshift evolution is stronger than for AGNs: The curve for E^{-2} in Fig. 7 corresponds to the evolution parameters $m=5$, $z_{\max}=3$ and $E_{\max}=10^{22}$ eV, the curve for $E^{-1.75}$ to $m=4.5$, $z_{\max}=3$ and $E_{\max}=10^{23}$ eV, and the curve for mono-energetic injection to $m=4$, $z_{\max}=3$, and $E_{\max}=10^{21}$ eV.

Figure 8 shows that between $\sim 10^{18}$ eV and $\sim 10^{20}$ eV the energy loss rate of protons on the CMB is dominated by pair production instead of pion production. The former does not contribute to neutrino production but the EM cascades initiated by the pairs lead to contributions to the diffuse γ-ray background in the GeV range. Thus, the cosmogenic neutrino flux is the more severely constrained the bigger the fraction of cosmic ray power is in the range $10^{18}\ \mathrm{eV}\lesssim E\lesssim 10^{20}$ eV. This is mostly important for soft injection spectra and explains why the total neutrino energy fluence decreases with increasing α in Fig. 7.

D. Comparison with experimental limits and future sensitivities

Figures 9 and 10 shows a scenario maximized over all 4 parameters in comparison to existing neutrino flux upper limits and expected sensitivities of future projects, respectively. Both of these fall into two groups, detection in water or ice or underground, typically sensitive below $\simeq 10^{16}$ eV, and air shower detection, usually sensitive at higher energies. Existing upper limits come from the underground MACRO experiment [11] at Gran Sasso, AMANDA [4] in the South Pole ice, and the Lake BAIKAL neutrino telescope [7] in the first category, and the AGASA ground array [30], the former fluorescence experiment Fly's Eye [29], the Radio Ice Cer-

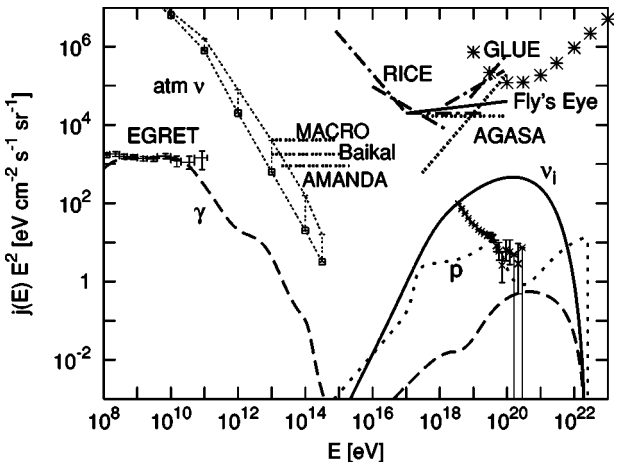

FIG. 9. A scenario with maximal cosmogenic neutrino fluxes as obtained by tuning the parameters to $z_{\max}=2$, $E_{\max}=10^{23}$ eV, $m=3$, $\alpha=1$. Also shown are predicted and observed cosmic ray and γ-ray fluxes, the atmospheric neutrino flux [65], as well as existing upper limits on the diffuse neutrino fluxes from MACRO [11], AMANDA [4], BAIKAL [7], AGASA [30], the Fly's Eye [29] and RICE [34] experiments, and the limit obtained with the Goldstone radio telescope (GLUE) [35], as indicated. The cosmic ray data are as in Fig. 1.

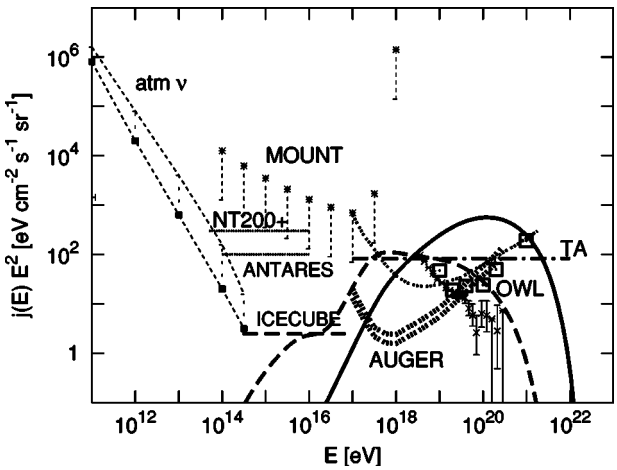

FIG. 10. The cosmogenic neutrino flux (solid line) shown in Fig. 9 in comparison with expected sensitivities of the currently being constructed Auger project to electron/muon and tau-neutrinos [28], and the planned projects telescope array (TA) [66] (dashed-dotted line), the fluorescence/Cerenkov detector MOUNT [32], and, indicated by squares, the space based OWL [67] (we take the latter as representative also for EUSO), the water-based NT200+ [7], ANTARES [9] (the NESTOR [10] sensitivity would be similar to ANTARES according to Ref. [12]), and the ice-based ICECUBE [5], as indicated. Also shown (dashed line) is an extreme scenario with $z_{\max}=3$, $E_{\max}=10^{22}$ eV, $m=5$, and $\alpha=2$, leading to a cosmogenic neutrino flux extending to relatively low energies where ANTARES and ICECUBE will be sensitive, and the atmospheric neutrino flux for comparison.

enkov Experiment RICE [34], and the Goldstone Lunar Ultrahigh energy neutrino experiment GLUE [35] in the second category. Future experiments in the first category include NT200+ at Lake Baikal [7], ANTARES in the Mediterranean [9], NESTOR in Greece [10], AMANDA-II [69], and ICECUBE [5], the next-generation version of AMANDA, whereas the air shower based category includes the Auger project [28], the Japanese telescope array [66], the fluorescence/Cerenkov detector MOUNT [32], and the space based OWL [67] and EUSO [24] experiments. The vertical bars for the MOUNT sensitivity characterize the uncertainties due to the not yet determined zenith angle range and sensitivity to the fluorescence component. The OWL sensitivity estimate is based on deeply penetrating atmospheric showers induced by electron or muon-neutrinos only [67] and may thus be considerably better if tau neutrinos, Cerenkov events, and Earth skimming events are taken into account [68]. The same applies to the EUSO project [24]. The AMANDA-II sensitivity will lie somewhere between the ANTARES and ICECUBE sensitivities [69]. The maximized fluxes shown in Figs. 9 and 10 are considerably higher than the ones discussed in Refs. [37,62,70–72], and should be easily detectable by at least some of these future instruments, as is obvious from Fig. 10.

IV. NEUTRINO FLUXES IN TOP-DOWN SCENARIOS

Historically, top-down scenarios were proposed as an alternative to acceleration scenarios to explain the huge energies up to 3×10^{20} eV observed in the cosmic ray spectrum [73]. In these top-down scenarios UHECRs are the decay products of some super-massive "X" particles of mass $m_X \gg 10^{20}$ eV close to the grand unified scale, and have energies all the way up to $\sim m_X$. Thus, the massive X particles could be metastable relics of the early Universe with lifetimes of the order the current age of the Universe or could be released from topological defects that were produced in the early Universe during symmetry-breaking phase transitions envisaged in grand unified theories (GUTs). The X particles typically decay into leptons and quarks. The quarks hadronize, producing jets of hadrons which, together with the decay products of the unstable leptons, result in a large cascade of energetic photons, neutrinos and light leptons with a small fraction of protons and neutrons, some of which contribute to the observed UHECR flux. The resulting injection spectra have been calculated from QCD in various approximations, see Ref. [14] for a review and Ref. [74] for more recent work. In the present work we will use the spectra shown in Fig. 11 which are obtained from solving the Dokshitzer-Gribov-Lipatov-Altarelli-Parisi (DGLAP) equations in the modified leading logarithmic approximation (MLLA) without supersymmetry for X particles decaying into two quarks, assuming 10% nucleons in the fragmentation spectrum. For dimensional reasons the spatially averaged X particle injection rate can only depend on the mass scale m_X and on cosmic time t in the combination

$$\dot{n}_X(t)=\kappa m_X^p t^{-4+p}, \tag{3}$$

where κ and p are dimensionless constants whose values depend on the specific top-down scenario [73]. Extragalactic topological defect sources usually predict $p=1$, whereas decaying super-heavy dark matter of lifetime much larger than

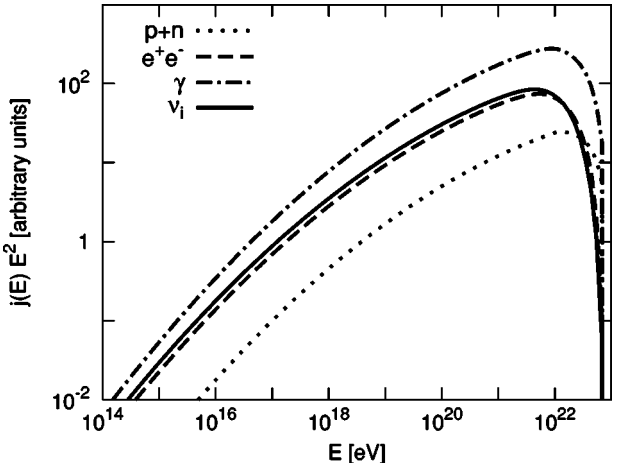

FIG. 11. Unnormalized nucleon, electron, γ-ray, and neutrino (per flavor) MLLA spectra resulting from X particles decaying into two quarks without supersymmetry. These spectra are used as injection spectra of top-down models in the present work. The spectra of antiparticles can be assumed identical.

the age of the Universe corresponds to $p=2$ [14]. In the latter case the observable flux will be dominated by decaying particles in the galactic halo and thus at distances smaller than all relevant interaction lengths. Composition and spectra will thus be directly given by the injection spectra which are most likely inconsistent with upper limits on the UHE photon fraction above 10^{19} eV [75], see Fig. 11. In addition, decaying dark matter scenarios suffer in general from a more severe fine tuning problem and predict a smaller neutrino flux than extragalactic topological defect model scenarios. We will therefore focus here on the latter, with $p=1$. Figure 12 shows the results for $m_X=2\times10^{14}$ GeV, with $B=10^{-12}$ G, and again the minimal URB consistent with data [58,76]. These parameters lead to optimistic neutrino fluxes for the maximal normalization consistent with all data. For more detailed recent discussions of top-down fluxes see Refs. [77,78].

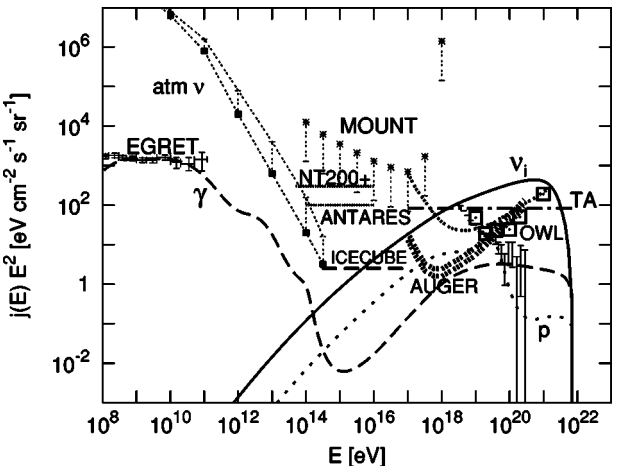

FIG. 12. Flux predictions for a TD model characterized by $p=1$, $m_X=2\times10^{14}$ GeV, and the injection spectra given in Fig. 11. The line key is as in Fig. 10.

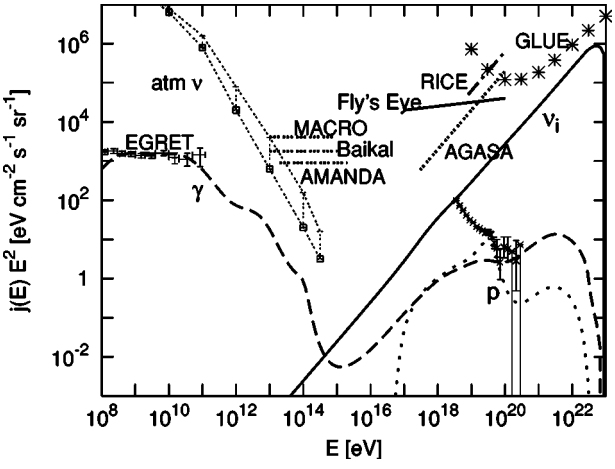

FIG. 13. Flux predictions for a *Z*-burst model averaged over flavors and characterized by the injection parameters $z_{\min}=0$, $z_{\max}=3$, $\alpha=1$, $m=0$, in Eq. (1) for neutrino primaries. All neutrino masses were assumed equal with $m_\nu=0.1$ eV and we again assumed maximal mixing between all flavors. The line key is as in Fig. 9.

V. THE *Z*-BURST SCENARIO WITH ACCELERATION SOURCES

In the *Z*-burst scenario UHECRs are produced by *Z*-bosons decaying within the distance relevant for the GZK effect. These *Z*-bosons are in turn produced by UHE neutrinos interacting with the relic neutrino background [45]. If the relic neutrinos have a mass m_ν, *Z*-bosons can be resonantly produced by UHE neutrinos of energy $E_\nu \simeq M_Z^2/(2m_\nu) \simeq 4.2\times10^{21}\,\mathrm{eV}\,(\mathrm{eV}/m_\nu)$. The required neutrino beams could be produced as secondaries of protons accelerated in high-redshift sources. The fluxes predicted in these scenarios have recently been discussed in detail in Refs. [46,79]. In Fig. 13 we show an optimistic example taken from Ref. [46] for comparison with the other scenarios. As in Refs. [46,79] no local neutrino over-density was assumed. The sources are assumed to not emit any γ rays, otherwise the *Z*-burst model with acceleration scenarios is ruled out, as demonstrated in Ref. [46]. We note that no known astrophysical accelerator exists that meets the requirements of the *Z*-burst model [46]. Also note that even exclusively emitting neutrino sources appear close to being ruled out already by the GLUE bound.

VI. MONO-ENERGETIC SUPER-HEAVY RELIC NEUTRINO SOURCES

Since no known astrophysical accelerator exists that produces sufficiently strong neutrino beams up to sufficiently high energies for the *Z*-burst scenario to work [46], one can speculate about more exotic sources. Gelmini and Kusenko [47] have considered a top-down type source for the *Z*-burst scenario, namely super-heavy particles mono-energetically decaying exclusively into neutrinos. In Fig. 14 we show predictions for one example of this kind of model with the same maximal energy $E_{\max}=10^{23}$ eV$=m_X/2$ as for case of the *Z*-burst model. Again, no local neutrino over-density was assumed and the calculation assumed a minimal URB flux and

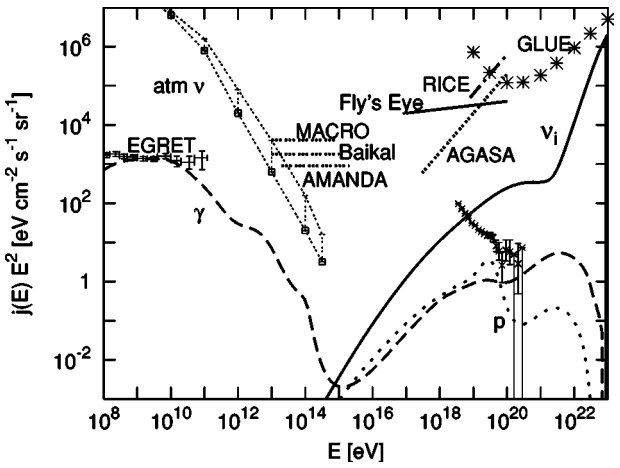

FIG. 14. Flux predictions for a Gelmini-Kusenko model characterized by $p=2$, $m_X=2\times10^{14}$ GeV in Eq. (3), with X particles exclusively decaying into neutrino–anti-neutrino pairs of all flavors (with equal branching ratio), assuming all neutrino masses $m_\nu=0.1$ eV. The line key is as in Fig. 9.

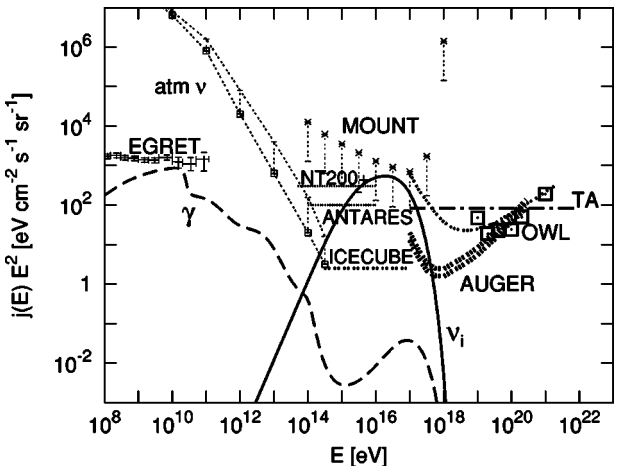

FIG. 15. Neutrino flux predictions for the AGN model [49] for a uniform distribution of blazars (no redshift evolution). The photon flux is below the measured EGRET value. The typical neutrino flux in this model contains the same energy as the photons. The position of the peak is governed by the initial proton distribution. The line key is as in Fig. 10.

a magnetic field $B=10^{-12}$ G. Note that, for the same UHECR flux, in this scenario the photon flux in the EGRET region is larger than in the *Z*-burst model with power-law neutrino sources, compare Fig. 13, because all secondary photons from *Z*-boson decays at redshifts $z>3$ contribute only to the EGRET energy range. Thus, the normalization of the photon flux to the EGRET measurements leads to a decrease of the UHE proton and photon fluxes, see Fig. 14. The EGRET measurement therefore considerably constrains the parameter space of this model. Neutrino masses $m_\nu \gg 0.1$ eV are required, which allow X-particle masses $m_X \lesssim 10^{14}$ GeV implying secondary photon fluxes that are below the measured level in the EGRET energy range.

Let us also note that though the neutrino flux in the UHECR region is much smaller in the Gelmini-Kusenko model in comparison with the *Z*-burst model, the GLUE bound constrains both models in the peak of neutrino flux in a similar way.

VII. NEUTRINO FLUXES IN A NON-SHOCK ACCELERATION MODEL FOR AGN

Although the recent exciting discoveries by the Chandra x-ray space observatory added much to our knowledge of structures of the jets of powerful radiogalaxies and quasars, they did not solve the old problems and, in fact, brought new puzzles. If the observed x-ray emission is due to synchrotron energy losses of electrons, the energy of such electrons should be of the order of 100 TeV. Electrons of such energies lose all their energy on a typical scale of only 0.1 kpc. In order to explain observed x-ray data, such 100 TeV electrons should be created uniformly over the jet length of order of 100 kpc. The conventional shock-wave acceleration mechanism in this case would require a jet uniformly filled with 1000 identical shocks, following one another along the jet axis.

In Ref. [49] a ''non-shock acceleration'' version of the electron synchrotron model was proposed, namely assuming that electrons are not accelerated in the jet, but are instead the result of pair production by very high energy (VHE) γ rays interacting with the CMB. The typical attenuation length of 10^{16-18} eV photons is of order 100 kpc, comparable with the lengths of large scale extragalactic jets.

In this model the VHE γ rays are produced by accelerated protons interacting with the ambient photon fields (supplied, for example by the accretion disk around the massive black hole) through photo-meson processes. At the same time those protons produce neutrinos which are emitted in the direction of the jet. Therefore, this model predicts a high neutrino flux comparable in power with the γ-ray flux. The detailed numerical simulations of proton acceleration in the central engine of the AGN [80] show that the collimated jet of almost mono-energetic VHE protons (linear accelerator) can be created in the electro-magnetic field around the black hole and the energy of those protons can be converted into photons and neutrinos, while protons can be captured inside of the source. The nucleon flux leaving the AGN is well below observed cosmic ray flux in this scenario. Furthermore, since all nucleons leaving the source are well below the GZK cutoff, there is no cosmogenic contribution to the neutrino flux from these sources.

Figure 15 shows a typical prediction of the diffuse neutrino flux in this scenario. This flux is beyond the WB limit which is not applicable in this case because the sources are optically thick for nucleons with respect to pion photoproduction. The flux is consistent with MPR bound for optically thick sources.

In the AGN model discussed above, blazars would be seen by neutrino telescopes as point-like sources with neutrino fluxes which are smaller or of the same order as the photon flux emitted by these same sources and which are detectable by γ-ray telescopes.

VIII. CONCLUSIONS

Based on our transport code we reconsidered neutrino flux predictions and especially their maxima consistent with all cosmic and γ-ray data, for cosmogenic neutrinos produced through pion production of UHECRs during propagation, and for the more speculative *Z*-burst scenario and top-down scenarios. We pointed out that one can easily exceed the WB bound and, in the most optimistic cases, even the MPR bound for cosmogenic neutrinos in scenarios with cosmic ray injection spectra harder than $E^{-1.5}$, maximal energies $E_{\rm max} \gtrsim 10^{22}$ eV, and redshift evolution typical for quasars, or stronger. Given our poor knowledge on the origin of UHECRs, in our opinion these are possibilities that should not be discarded at present, especially since they would lead to considerably increased prospects of ultrahigh energy neutrino detection in the near future. We also show that for non-shock AGN acceleration models the AGN neutrino fluxes can reach the γ-ray bound Eq. (2) around 10^{16} eV which represents the ultimate limit for all scenarios of γ-ray and neutrino production involving pion production.

Finally, we note that fluxes as high as for the optimistic scenarios discussed here would also lead to much stronger constraints on the neutrino-nucleon cross section at energies beyond the electroweak scale. This is important, for example, in the context of theories with extra dimensions and a fundamental gravity scale in the TeV range [81].

ACKNOWLEDGMENTS

We would like to thank Andrey Neronov and Igor Tkachev for fruitful discussions and comments. We thank Cyrille Barbot, Zoltan Fodor, and Andreas Ringwald for useful comments on the first version of the manuscript. We also thank David Seckel for information on the RICE experiment.

[1] For a recent paper on the implications of the neutrinos detected from SN 1987A for oscillation parameters see, e.g., M. Kachelriess, A. Strumia, R. Tomas, and J.W. Valle, Phys. Rev. D **65**, 073016 (2002).

[2] For reviews see, e.g., R.J. Protheroe, Nucl. Phys. B (Proc. Suppl.) **77**, 456 (1999); R. Gandhi, *ibid.* **91**, 453 (2000); J.G. Learned and K. Mannheim, Annu. Rev. Nucl. Part. Sci. **50**, 679 (2000).

[3] For general information see http://amanda.berkeley.edu/; see also F. Halzen, New Astron. Rev. **42**, 289 (1999); for the newest status see, e.g., AMANDA Collaboration, G.C. Hill *et al.*, astro-ph/0106064.

[4] AMANDA Collaboration, M. Kawalski *et al.*, hep-ph/0112083, Proceedings of the EPS International Conference on High Energy Physics, Budapest, 2001, edited by D. Horvath, P. Levai, and A. Patkos, JHEP Proceedings Section, PrHEP-hep2001/207.

[5] For general information see http://www.ps.uci.edu/~icecube/workshop. html; see also F. Halzen, Am. Astron. Soc. Meeting 192,#62 28 (1998); AMANDA Collaboration, E. Andres *et al.*, in Proc. 8th International Workshop on Neutrino Telescopes, Venice, 1999, astro-ph/9906705.

[6] For general information see http://www-zeuthen.desy.de/baikal/baikalhome.html; see also Baikal Collaboration, V. Balkanov *et al.*, in Proceedings of the IX International Workshop on Neutrino Telescopes, Venezia, edited by M. Balda-Ceolin, Vol. II, p. 591.

[7] BAIKAL Collaboration, V. Balkanov *et al.*, Nucl. Phys. B (Proc. Suppl.) **110**, 504 (2002).

[8] Proc. 19th Texas Symposium on Relativistic Astrophysics, Paris (France), edited by E. Aubourg *et al.* [Nucl. Phys. B (Proc. Suppl.) **80B** (2000)].

[9] For general information see http://antares.in2p3.fr; see also S. Basa, in Ref. [8], astro-ph/9904213; ANTARES Collaboration, E. Aslanides *et al.*, astro-ph/9907432.

[10] For general information see http://www.nestor.org.gr. See also L. Resvanis, Proc. Int. Workshop on Neutrino Telescopes, Venice, 1999, Vol. II, p. 93.

[11] For general information see http://wsgs02.lngs.infn.it:8000/macro/; see also MACRO Collaboration, M. Ambrosio *et al.*, astro-ph/0203181.

[12] C. Spiering, Prog. Part. Nucl. Phys. **48**, 43 (2002); F. Halzen and D. Hooper, astro-ph/0204527.

[13] For recent reviews see J.W. Cronin, Rev. Mod. Phys. **71**, S165 (1999); M. Nagano and A.A. Watson, *ibid.* **72**, 689 (2000); A.V. Olinto, Phys. Rep. **333**, 329 (2000); X. Bertou, M. Boratav, and A. Letessier-Selvon, Int. J. Mod. Phys. A **15**, 2181 (2000).

[14] P. Bhattacharjee and G. Sigl, Phys. Rep. **327**, 109 (2000); see also G. Sigl, Science **291**, 73 (2001), for a short review.

[15] K. Greisen, Phys. Rev. Lett. **16**, 748 (1966); G.T. Zatsepin and V.A. Kuzmin, Pis'ma Zh. Eksp. Theor. **4**, 114 (1966) [JETP Lett. **4**, 78 (1966)].

[16] D.J. Bird *et al.*, Phys. Rev. Lett. **71**, 3401 (1993); Astrophys. J. **424**, 491 (1994); **441**, 144 (1995).

[17] See, e.g., M.A. Lawrence, R.J. Reid, and A.A. Watson, J. Phys. G **17**, 733 (1991), and references therein; see also http://ast.leeds.ac.uk/haverah/hav-home.html.

[18] N.N. Efimov *et al.*, in *Proceedings of the International Symposium on Astrophysical Aspects of the Most Energetic Cosmic Rays*, edited by M. Nagano and F. Takahara (World Scientific, Singapore, 1991), p. 20; B.N. Afnasiev, in *Proceedings of the International Symposium on Extremely High Energy Cosmic Rays: Astrophysics and Future Observatories*, edited by M. Nagano (Institute for Cosmic Ray Research, Tokyo, 1996), p. 32.

[19] M. Takeda *et al.*, Phys. Rev. Lett. **81**, 1163 (1998); see N. Hayashida *et al.*, Astrophys. J. **522**, 225 (1999); for an update; see also http://www-akeno.icrr.u-tokyo.ac.jp/AGASA/.

[20] D. Kieda *et al.*, Proc. of the 26th ICRC, Salt Lake, 1999; http://www.physics.utah.edu/Resrch.html.

[21] Talk on the 27th ICRC, Hamburg, 2001.

[22] J.W. Cronin, Nucl. Phys. B (Proc. Suppl.) **28B**, 213 (1992); The Pierre Auger Observatory Design Report, 2nd ed., 1997; see also http://www.auger.org/ and http://www-lpnhep.in2p3.fr/auger/welcome.html

[23] M. Teshima *et al.*, Nucl. Phys. B (Proc. Suppl.) **28B**, 169 (1992); see also http://www-ta.icrr.u-tokyo.ac.jp/
[24] See http://www.ifcai.pa.cnr.it/Ifcai/euso.html.
[25] *Proceedings of the 25th International Cosmic Ray Conference*, edited by M.S. Potgieter *et al.* (Durban, 1997).
[26] *Proceedings of the International Symposium on Extremely High Energy Cosmic Rays: Astrophysics and Future Observatories*, edited by M. Nagano (Institute for Cosmic Ray Research, Tokyo, 1996).
[27] J.F. Ormes *et al.*, in [25], Vol. 5, 273; Y. Takahashi *et al.*, in [26], p. 310; see also http://lheawww.gsfc.nasa.gov/docs/gamcosray/hecr/OWL/.
[28] J.J. Blanco-Pillado, R.A. Vazquez, and E. Zas, Phys. Rev. Lett. **78**, 3614 (1997); K.S. Capelle, J.W. Cronin, G. Parente, and E. Zas, Astropart. Phys. **8**, 321 (1998); A. Letessier-Selvon, Nucl. Phys. B (Proc. Suppl.) **91**, 473 (2000); X. Bertou, P. Billoir, O. Deligny, C. Lachaud, and A. Letessier-Selvon, Astropart. Phys. **17**, 183 (2002).
[29] R.M. Baltrusaitis *et al.*, Astrophys. J. Lett. **281**, L9 (1984); Phys. Rev. D **31**, 2192 (1985).
[30] S. Yoshida for the AGASA Collaboration, Proc. of 27th ICRC (Hamburg) Vol. 3, p. 1142 (2001).
[31] See, e.g., D. Fargion, hep-ph/0111289.
[32] G.W.S. Hou and M.A. Huang, astro-ph/0204145.
[33] *Proceedings of First International Workshop on Radio Detection of High-Energy Particles*, Los Angeles, California, 2000, edited by D. Saltzberg and P. Gorham, AIP Conf. Proc. No. 579 (AIP, Melville, NY, 2001), and at http://www.physics.ucla.edu/moonemp/radhep/workshop.html.
[34] RICE Collaboration, I. Kravchenko *et al.*, astro-ph/0206371; for general information on RICE see http://kuhep4.phsx.ukans.edu/iceman/index.html.
[35] P.W. Gorham, K.M. Liewer, and C.J. Naudet, astro-ph/9906504; P.W. Gorham, K.M. Liewer, C.J. Naudet, D.P. Saltzberg, and D.R. Williams, astro-ph/0102435, in Ref. [33].
[36] See, e.g., L.G. Dedenko, I.M. Zheleznykh, S.K. Karaevsky, A.A. Mironovich, V.D. Svet, and A.V. Furduev, Izv. Ross. Akad. Nauk, Ser. Fiz. **61**, 593 (1997) [Bull. Russ. Acad. Sci. Phys. **61**, 469 (1997)].
[37] V.S. Beresinsky and G.T. Zatsepin, Phys. Lett. **28B**, 423 (1969); V.S. Berezinsky and G.T. Zatsepin, Yad. Fiz. **11**, 200 (1970) [Sov. J. Nucl. Phys. **11**, 111 (1970)].
[38] G.R. Farrar and P.L. Biermann, Phys. Rev. Lett. **81**, 3579 (1998); C.M. Hoffman, *ibid.* **83**, 2471 (1999); G.R. Farrar and P.L. Biermann, *ibid.* **83**, 2472 (1999); G. Sigl, D.F. Torres, L.A. Anchordoqui, and G.E. Romero, Phys. Rev. D **63**, 081302(R) (2001); A. Virmani *et al.*, Astropart. Phys. **17**, 489 (2002).
[39] P.G. Tinyakov and I.I. Tkachev, Pis'ma Zh. Eksp. Teor. Fiz. **74**, 499 (2001) [JETP Lett. **74**, 445 (2001)]; astro-ph/0111305; see also Pis'ma Zh. Eksp. Teor. Fiz. **74**, 3 (2001) [JETP Lett. **74**, 1 (2001)].
[40] D.S. Gorbunov, P.G. Tinyakov, I.I. Tkachev, and S.V. Troitsky, astro-ph/0204360.
[41] V. Berezinsky, A.Z. Gazizov, and S.I. Grigorieva, hep-ph/0204357.
[42] O.E. Kalashev, V.A. Kuzmin, D.V. Semikoz, and I.I. Tkachev, astro-ph/0107130.
[43] D.J. Chung, G.R. Farrar, and E.W. Kolb, Phys. Rev. D **57**, 4606 (1998); D.S. Gorbunov, G.G. Raffelt, and D.V. Semikoz, *ibid.* **64**, 096005 (2001).
[44] V.A. Kuzmin and I.I. Tkachev, Phys. Rep. **320**, 199 (1999).
[45] T.J. Weiler, Phys. Rev. Lett. **49**, 234 (1982); Astrophys. J. **285**, 495 (1984); Astropart. Phys. **11**, 303 (1999); D. Fargion, B. Mele, and A. Salis, Astrophys. J. **517**, 725 (1999); S. Yoshida, G. Sigl, and S.j. Lee, Phys. Rev. Lett. **81**, 5505 (1998).
[46] O.E. Kalashev, V.A. Kuzmin, D.V. Semikoz, and G. Sigl, Phys. Rev. D **65**, 103003 (2002).
[47] G. Gelmini and A. Kusenko, Phys. Rev. Lett. **84**, 1378 (2000).
[48] V. Berezinsky, M. Kachelriess, and S. Ostapchenko, hep-ph/0205218.
[49] A. Neronov, D. Semikoz, F. Aharonian, and O. Kalashev, Phys. Rev. Lett. **89**, 051101 (2002).
[50] S. Lee, Phys. Rev. D **58**, 043004 (1998); see also Ref. [14].
[51] O.E. Kalashev, V.A. Kuzmin, and D.V. Semikoz, astro-ph/9911035; Mod. Phys. Lett. A **16**, 2505 (2001).
[52] P.S. Coppi and F.A. Aharonian, Astrophys. J. Lett. **487**, L9 (1997).
[53] P. Sreekumar *et al.*, Astrophys. J. **494**, 523 (1998).
[54] E. Waxman and J.N. Bahcall, Phys. Rev. D **59**, 023002 (1999); J.N. Bahcall and E. Waxman, *ibid.* **64**, 023002 (2001).
[55] K. Mannheim, R.J. Protheroe, and J.P. Rachen, Phys. Rev. D **63**, 023003 (2001); J.P. Rachen, R.J. Protheroe, and K. Mannheim, astro-ph/9908031, in Ref. [8].
[56] T. Sjostrand, Comput. Phys. Commun. **82**, 74 (1994).
[57] OPAL Collaboration, G. Alexander *et al.*, Z. Phys. C **69**, 543 (1996).
[58] R.J. Protheroe and P.L. Biermann, Astropart. Phys. **6**, 45 (1996); **7**, 181 (1996).
[59] J.R. Primack, R.S. Somerville, J.S. Bullock, and J.E. Devriendt, astro-ph/0011475.
[60] Super-Kamiokande Collaboration, Y. Fukuda *et al.*, Phys. Rev. Lett. **81**, 1562 (1998); SNO Collaboration, Q.R. Ahmad *et al.*, *ibid.* **87**, 071301 (2001).
[61] B.J. Boyle and R.J. Terlevich, Mon. Not. R. Astron. Soc. **293**, L49 (1998).
[62] R. Engel, D. Seckel, and T. Stanev, Phys. Rev. D **64**, 093010 (2001).
[63] E. Boldt and P. Ghosh, Mon. Not. R. Astron. Soc. **307**, 491 (1999); A. Levinson, Phys. Rev. Lett. **85**, 912 (2000); E. Boldt and M. Lowenstein, Mon. Not. R. Astron. Soc. **316**, L29 (2000).
[64] S.A. Colgate, Phys. Scr., T **T52**, 96 (1994).
[65] See, e.g., P. Lipari, Astropart. Phys. **1**, 195 (1993).
[66] M. Sasaki and M. Jobashi, astro-ph/0204167.
[67] See http://www.fcp01.vanderbilt.edu/schedules/upload/John_Krizmanic-OWL-vandy.pdf; see also D.B. Cline and F.W. Stecker, OWL/AirWatch science white paper, astro-ph/0003459.
[68] A. Kusenko and T.J. Weiler, Phys. Rev. Lett. **88**, 161101 (2002); J.L. Feng, P. Fisher, F. Wilczek, and T.M. Yu, *ibid.* **88**, 161102 (2002).
[69] See AMANDA Collaboration, R. Wischnewski, astro-ph/0204268.
[70] F.W. Stecker, Astrophys. J. **228**, 919 (1979).

[71] R.J. Protheroe and P.A. Johnson, Astropart. Phys. **4**, 253 (1996).
[72] S. Yoshida, H.y. Dai, C.C. Jui, and P. Sommers, Astrophys. J. **479**, 547 (1997).
[73] P. Bhattacharjee, C.T. Hill, and D.N. Schramm, Phys. Rev. Lett. **69**, 567 (1992).
[74] N. Rubin, M. Ph. thesis, Cavendish Laboratory, University of Cambridge, 1999, http://www.stanford.edu/nrubin/Thesis.ps; Z. Fodor and S.D. Katz, Phys. Rev. Lett. **86**, 3224 (2001); S. Sarkar and R. Toldra, Nucl. Phys. **B621**, 495 (2002); C. Barbot and M. Drees, Phys. Lett. B **533**, 107 (2002).
[75] M. Ave, J.A. Hinton, R.A. Vazquez, A.A. Watson, and E. Zas, Phys. Rev. D **65**, 063007 (2002).
[76] T.A. Clark, L.W. Brown, and J.K. Alexander, Nature (London) **228**, 847 (1970).
[77] G. Sigl, S. Lee, D.N. Schramm, and P. Coppi, Phys. Lett. B **392**, 129 (1997).
[78] G. Sigl, S. Lee, P. Bhattacharjee, and S. Yoshida, Phys. Rev. D **59**, 043504 (1999).
[79] Z. Fodor, S.D. Katz, and A. Ringwald, Phys. Rev. Lett. **88**, 171101 (2002); hep-ph/0105336; J. High Energy Phys. **06**, 046 (2002); A. Ringwald, hep-ph/0111112.
[80] A. Neronov and D. Semikoz (in preparation).
[81] See, e.g., L.A. Anchordoqui, J.L. Feng, H. Goldberg, and A.D. Shapere, hep-ph/0112247; M. Kowalski, A. Ringwald, and H. Tu, Phys. Lett. B **529**, 1 (2002); A. Ringwald and H. Tu, *ibid.* **525**, 135 (2002).